European Journal of Mechanics B/Fluids 28 (2009) 146–151

Contents lists available at ScienceDirect

European Journal of Mechanics B/Fluids

www.elsevier.com/locate/ejmflu

A linear dispersive mechanism for numerical error growth: spurious caustics

Cl. David [a,*], P. Sagaut [a], T. Sengupta [b]

[a] Université Pierre et Marie Curie-Paris 6, Institut Jean Le Rond d'Alembert, UMR CNRS 7190, Boîte courrier n° 0162, 4, place Jussieu, F-75252 Paris cedex 05, France
[b] Indian Institute of Technology Kanpur, Department of Aerospace Engineering, U.P. 208016, India

ARTICLE INFO

Article history:
Received 25 September 2007
Received in revised form 12 March 2008
Accepted 23 April 2008
Available online 27 April 2008

Keywords:
Dispersion
Numerical schemes
Spurious caustics

ABSTRACT

A linear dispersive mechanism leading to a burst in the L_∞ norm of the error in numerical simulation of polychromatic solutions is identified. This local error pile-up corresponds to the existence of spurious caustics, which are allowed by the dispersive nature of the numerical error. From the mathematical point of view, spurious caustics are related to extrema of the numerical group velocity and are physically associated to interactions between rays defined by the characteristic lines of the discrete system. Several popular schemes are analyzed and are shown to admit spurious caustics. It is also observed that caustic-free schemes can be defined, like the Crank–Nicolson scheme.

1. Introduction

The analysis and the control of numerical error in discretized propagation-type equations is of major importance for both theoretical analysis and practical applications. A huge amount of works has been devoted to the analysis of the numerical errors, its dynamics and its influence on the computed solution (the reader is referred to classical books, among which [2,5,6,10]). It appears that existing works are mostly devoted to linear, one-dimensional numerical models, such as the linear advection equation

$$\frac{\partial u}{\partial t} + c\frac{\partial u}{\partial x} = 0 \tag{1}$$

where c is a constant uniform advection velocity. A striking observation is that, despite the tremendous efforts devoted to the analysis of numerical schemes in this simple case, the full exact non-homogeneous error equation has been derived only very recently [9].

The two sources of numerical error are the dispersive and dissipative properties of the numerical scheme, which are very often investigated in unbounded or periodic domains thanks to a spectral analysis. Following this approach, a monochromatic wave is used to measure the accuracy of the scheme. Such a tool is very powerful and provides the user with a deep insight into the discretization errors. But some results coming from practical numerical experiments still remain unexplained, despite the linear character of the discrete numerical model. As an example, let us note the sudden growth of the numerical error for long range propagation reported by Zingg [12] for a large set of numerical schemes, including optimized numerical schemes.

The usual modal analysis is almost always applied to monochromatic reference solutions, with the purpose of analyzing the error committed on both their amplitude and their phase, leading to classical plots of the relative error as the function of the Courant number and/or the number of grid points per wavelength. Therefore, dispersive phenomena associated to polychromatic solutions are usually not taken into account. It is also to be noted that the extension to bounded domains thanks to a Fourier–Laplace transform has recently been proposed [8,9].

A very interesting work reports on the dispersion and dissipation properties of numerical schemes [1], where, in the specific case of the advection of a step function, the solutions of the equivalent equation can be calculated by means of generalized Airy functions, which enable one to recover the numerical solution. Unfortunately, this method cannot be applied to the characterization of spurious caustics, in so far as those functions do not have bursting maxima.

The present paper deals with the analysis of a linear dispersive mechanism which results in local error focusing, i.e. to a sudden local error burst in the L_∞ norm for polychromatic solutions. This phenomena is reminiscent of the physical one referred to as the caustic phenomenon in linear dispersive physical models [11], and will be referred to as the spurious caustic phenomenon hereafter. It will be shown that, for some specific values of the Courant number, spurious caustics can exist for some popular finite-difference schemes. The present analysis is restricted to interior stencil, and the influence of boundary conditions will not be considered.

The paper is organized as follows. The numerical schemes retained for the present analysis are briefly recalled in Section 2. Main elements of caustic theory of interest for the present analy-

* Corresponding author.
E-mail address: david@lmm.jussieu.fr (Cl. David).

0997-7546/$ – see front matter
doi:10.1016/j.euromechflu.2008.04.002

Table 1
Numerical scheme coefficients

Name	α	β	γ	δ	ϵ	ζ	η	θ	υ
Leapfrog	$\frac{1}{2\tau}$	0	$\frac{-1}{2\tau}$	$\frac{c}{2h}$	$\frac{-c}{2h}$	0	0	0	0
Lax	$\frac{1}{\tau}$	0	0	$\frac{-1}{2\tau}+\frac{c}{2h}$	$\frac{-1}{2\tau}-\frac{c}{2h}$	0	0	0	0
Lax–Wendroff	$\frac{1}{\tau}$	$\frac{-1}{\tau}+\frac{c^2\tau}{h^2}$	0	$\frac{(1-\sigma)c}{2h}$	$\frac{-(1+\sigma)c}{2h}$	0	0	0	0
Crank–Nicolson	$\frac{2}{\tau}$	$\frac{2}{\tau}$	0	$\frac{-c}{2h}$	$\frac{c}{2h}$	$\frac{c}{2h}$	0	$\frac{-c}{2h}$	0

sis are briefly recalled in Section 3. Test schemes are analyzed in Section 4.

2. Test numerical schemes

For the sake of simplicity, the analysis will be restricted to schemes which involves at most three time levels and three grid points. The extension of the present analysis to other schemes is straightforward. For this class of schemes, the general finite-differenced version of the linear advection equation (1) can therefore be written as follows

$$\alpha u_j^{n+1}+\beta u_j^n+\gamma u_j^{n-1}+\zeta u_{j+1}^{n+1}+\delta u_{j+1}^n+\upsilon u_{j+1}^{n-1}+\theta u_{j-1}^{n+1}+\varepsilon u_{j-1}^n+\eta u_{j-1}^{n-1}=0 \tag{2}$$

with

$$u_l{}^m = u(lh, m\tau) \tag{3}$$

where h and τ are the mesh size and time step respectively. For the sake of simplicity, these two quantities are assumed to be uniform. The CFL number is defined as $\sigma = c\tau/h$, while the non-dimensional wave number is defined as $\varphi = kh$, where k is the wave number of the signal under consideration.

A numerical scheme is specified by selecting appropriate values of the coefficients α, β, γ, δ, ε, ζ, η, υ and θ in Eq. (2). Values corresponding to numerical schemes retained for the present works are given in Table 1.

3. Caustics

3.1. Analytical validation

The solution of Eq. (1) is taken under the form:

$$u(x,t,k) = e^{i(kx-\omega t)} \tag{4}$$

where $\omega = \xi_\omega + i\eta_\omega$ is the complex phase, and k the real wave number. For dispersive waves, it is recalled that the group velocity $V_g(k)$ is defined as

$$V_g(k) \equiv \frac{\partial \xi_\omega}{\partial k} \tag{5}$$

A caustic is defined as a focusing of different rays in a single location. The equivalent condition is that the group velocity exhibits an extremum, i.e. there exists at least one wave number k_c such that

$$\frac{\partial V_g}{\partial k}(k_c) = 0 \tag{6}$$

The corresponding physical interpretation is that wave packets with characteristic wave numbers close to k_c will pile-up after a finite time and will remain superimposed for a long time, resulting in the existence a region of high energy followed by a region with very low fluctuation level.

The linear continuous model equation (1) is not dispersive if the convection velocity c is uniform, and therefore the exact solution does not exhibits caustics since the group velocity does not depend on k. The discrete solution associated with a given numerical scheme will admit spurious caustics, and therefore spurious local energy pile-up and local sudden growth of the error, if the discrete dispersion relation is such that the condition (6) is satisfied. For a uniform scale-dependent convection velocity, such spurious caustics can exist in polychromatic solutions only, since they are associated to the superposition of wave packets with different characteristic wave numbers.

The general dispersion relation associated with the discrete scheme (2) is

$$\alpha e^{i\varphi}+\zeta e^{2i\varphi}+\left(\beta e^{i\varphi}+\delta e^{2i\varphi}+\varepsilon\right)e^{i\omega dt}+\left(\gamma e^{i\varphi}+\eta\right)e^{2idt\omega}+\theta=0 \tag{7}$$

which is a non-linear quadratic equation in $e^{i\omega\tau}$ that can easily been solved.

The corresponding group velocity is given by:

$$V_g = h\frac{\partial \xi_\omega}{\partial \varphi} \tag{8}$$

The numerical solution will therefore admits spurious caustics if

$$\frac{\partial V_g}{\partial k} = \frac{\partial V_g}{\partial \varphi}\frac{\partial \varphi}{\partial k} = 0 \quad\Longleftrightarrow\quad \frac{\partial V_g}{\partial \varphi} = 0 \tag{9}$$

The corresponding values of φ and k will be respectively denoted φ_c and k_c.

Spurious caustics are associated with characteristic lines given by

$$\frac{x}{t} = U_c \tag{10}$$

where

$$U_c = V_g(\varphi_c) \tag{11}$$

We now illustrate the caustic phenomenon considering the two following sinusoidal wave packets:

$$u_1 = e^{-\alpha(x-x_0^1-ct)^2}\,\mathrm{Cos}\left[k_1\left(x-x_0^1-ct\right)\right] \tag{12}$$

$$u_2 = e^{-\alpha(x-x_0^2-ct)^2}\,\mathrm{Cos}\left[k_2\left(x-x_0^2-ct\right)\right] \tag{13}$$

where $\alpha > 0$. The two wave packets are initially centered at x_0^1 and x_0^2, respectively. The group velocity of the two wave packets are $V_1 = V_g(k_1)$ and $V_2 = V_g(k_2)$, respectively, where the function $V_g(x)$ is associated to the numerical scheme used to solve Eq. (1).

If the solution obeys the linear advection law given by Eq. (1), the initial field is passively advected at speed c, while, if the advection speed is scale-dependent (as in numerical solutions), the two packets will travel at different speeds, leading to the rise of discrepancies with the constant-speed solution. Another dispersive error is the shape-deformation phenomenon: due to numerical errors, the exact shape of the wave packets will not be exactly preserved. This secondary effect will not be considered below, since it is not related to the existence of spurious caustics. It is emphasized here that the occurrence of spurious caustics originates in the differential error in the group velocity, not in the fact that shapes of the envelope of the wave packets are not preserved. The issue of deriving shape-preserving schemes for passive scalar advection has been addressed by several authors (e.g. [3,4]).

The spurious caustics will appear if the two wave packets happen to get superimposed. During the cross-over, the L_∞ norm of the error (defined as the difference between the constant-speed solution and the dispersive one) will exhibit a maximum. The characteristic life time of the caustic, t^*, depends directly on the difference between the advection speeds of the two wave packets and the wave packet widths. Denoting l_1 and l_2 the characteristic length of the two wave packets, the time during which they will be (at least partially) superimposed can be estimated as

$$t^* = \frac{l_1+l_2}{|V_1-V_2|} \tag{14}$$

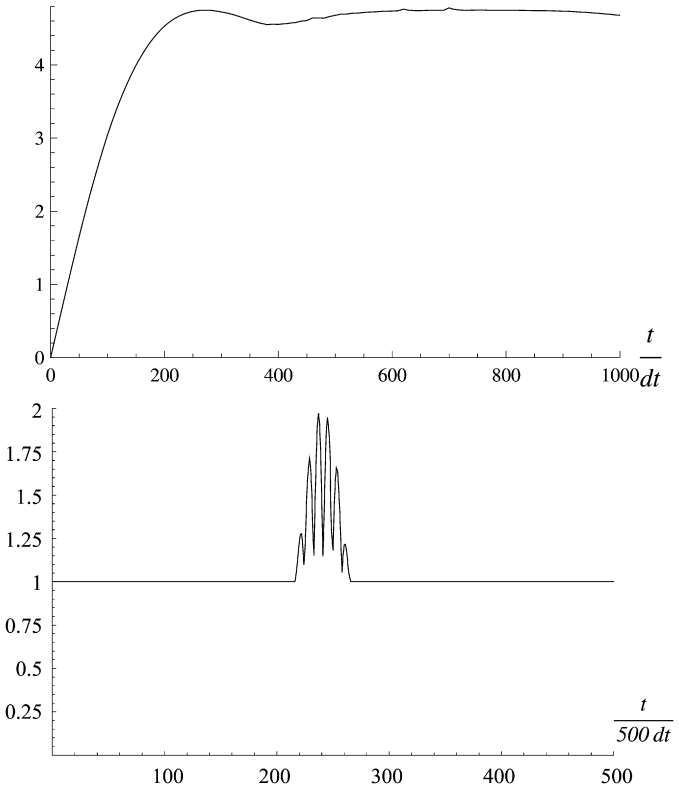

Fig. 1. Time history of the numerical error for the two-wave packet problem (shape deformation and dissipative errors are neglected to emphasize the linear focusing phenomenon). Top: L_1 norm. Bottom: L_∞ norm. Numerical parameters are $\alpha = 1$, $h = 0.01$, $V_1 = 2.04$, $V_2 = 2.02$, corresponding to the properties of the Lax scheme for $\sigma = 0.7$.

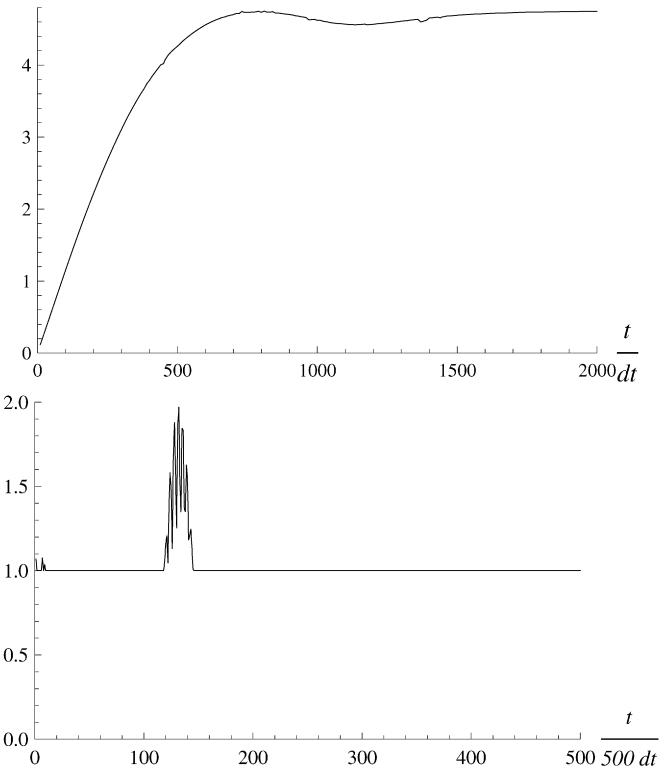

Fig. 2. Time history of the numerical error for the two-wave packet problem (shape deformation and dissipative errors are neglected to emphasize the linear focusing phenomenon). Top: L_1 norm. Bottom: L_∞ norm. parameters are $\alpha = 1$, $h = 0.01$, $V_1 = 0.66$, $V_2 = 0.63$, corresponding to the properties of the Lax–Wendroff scheme for $\sigma = 0.7$.

It is seen that, since caustics are defined as solutions for which $\partial V_g/\partial k = 0$, t^* will be large if $|k_1 - k_2| \ll 1$. Noting $k_1 = k_c + \delta k$ and $k_2 = k_c - \delta k$, one obtains

$$t^* \simeq \frac{l_1 + l_2}{2(\delta k)^2 |\frac{\partial^2 V_g}{\partial k}(k_c)|} \tag{15}$$

leading to $t^* \propto (\delta k)^{-2}$.

Neglecting shape-deformation effects and assuming that the numerical scheme is non-dissipative, the numerical error E is given by:

$$\begin{aligned} E = \big| & e^{-\alpha(x-x_0^1-ct)^2}\,\mathrm{Cos}\big[k_1(x-x_0^1-ct)\big] \\ & - e^{-\alpha(x-x_0^1-tV_1)^2}\,\mathrm{Cos}\big[k_1(x-x_0^1-tV_1)\big] \\ & + e^{-\alpha(x-x_0^2-ct)^2}\,\mathrm{Cos}\big[k_2(x-x_0^2-ct)\big] \\ & - e^{-\alpha(x-x_0^2-tV_2)^2}\,\mathrm{Cos}\big[k_2(x-x_0^2-tV_2)\big]\big| \end{aligned} \tag{16}$$

A simple analysis show that

$$\begin{aligned} & \lim_{t\to+\infty} L_\infty\big(E(t)\big) = L_\infty\big(u_1(t=0)\big), \\ & \max_t L_\infty\big(E(t)\big) = 2L_\infty\big(u_1(t=0)\big) \end{aligned} \tag{17}$$

The time histories of the L_1 and L_∞ norms of E for the Lax scheme, Lax–Wendroff scheme, and Leapfrog scheme, are respectfully displayed in Figs. 1–3, showing the occurrence of the caustic and the sudden growth of the L_∞ error norm.

3.2. Numerical validation

The advection of an exact solution of the transport equation (1) under the latter schemes, enables us to obtain numerical caustics.

Figs. 4–6 respectively display the isovalues of the residual kinetic energy for the Lax, Lax–Wendroff and Leapfrog schemes, for $cfl = 0.9$. Minima are in black, maxima in white. In each case, the caustic corresponds to the white domain, where the residual kinetic energy is maximal.

4. Analysis of test numerical schemes

We analyzed the properties of the numerical scheme displayed in Section 2.

For the Leapfrog scheme, the dispersion relation is:

$$1 - e^{2i\omega\tau} + 2i\sigma\,\mathrm{Sin}[\varphi]e^{i\omega\tau} = 0 \tag{18}$$

from which it comes that

$$e^{\eta_\omega \tau} = 1 \quad \Longrightarrow \quad \eta_\omega = 0 \tag{19}$$

$$\xi_\omega \tau = \mathrm{ArcSin}[\sigma\varphi] \tag{20}$$

The group velocity can be expressed as

$$V_g = \pm \frac{c\,\mathrm{Cos}[\varphi]}{\sqrt{1 - \sigma^2\,\mathrm{Sin}^2[\varphi]}} \tag{21}$$

leading to

$$\frac{\partial V_g}{\partial \varphi} = \frac{ch\,\mathrm{Sin}[\varphi]}{\sqrt{1 - \sigma^2\,\mathrm{Sin}^2[\varphi]}} \left(\frac{\sigma^2\,\mathrm{Cos}^2[\varphi]}{(1 - \sigma^2\,\mathrm{Sin}^2[\varphi])} - 1 \right) \tag{22}$$

A trivial root is $\varphi = 0 \bmod \pi$, which corresponds to

$$U_c = \pm c \tag{23}$$

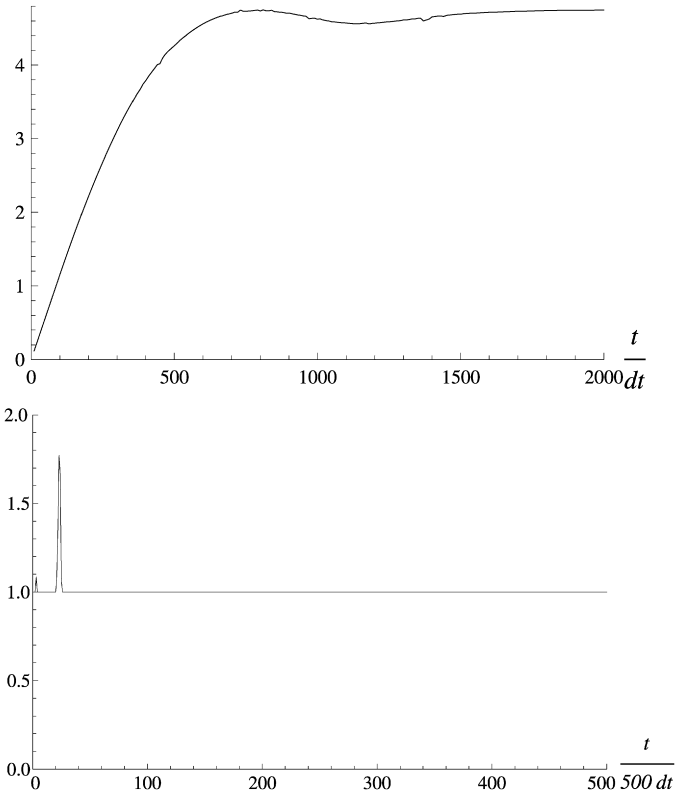

Fig. 3. Time history of the numerical error for the two-wave packet problem (shape deformation and dissipative errors are neglected to emphasize the linear focusing phenomenon). Top: L_1 norm. Bottom: L_∞ norm. Numerical parameters are $\alpha = 1$, $h = 0.01$, $V_1 = 0.022$, $V_2 = -0.11$, corresponding to the properties of the Leapfrog scheme for $\sigma = 0.7$.

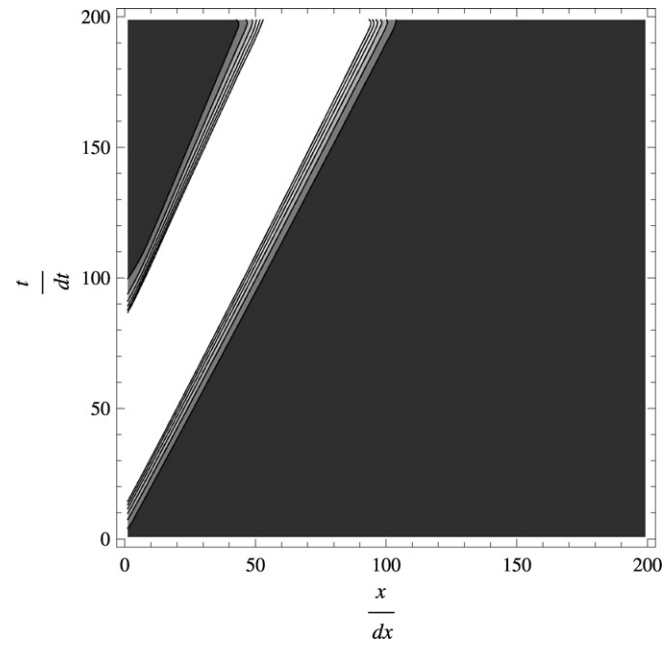

Fig. 4. Isovalues of the residual kinetic energy for the Lax scheme, for $cfl = 0.9$.

The existence of two convection speeds with opposite sign is due to the existence of two modes for the Leapfrog schemes: a physical and a computational mode with both having identical amplification factor but opposite group velocity (see e.g. [7]). Zeros of Eq. (22) in the (σ, φ) plane are displayed in Fig. 7.

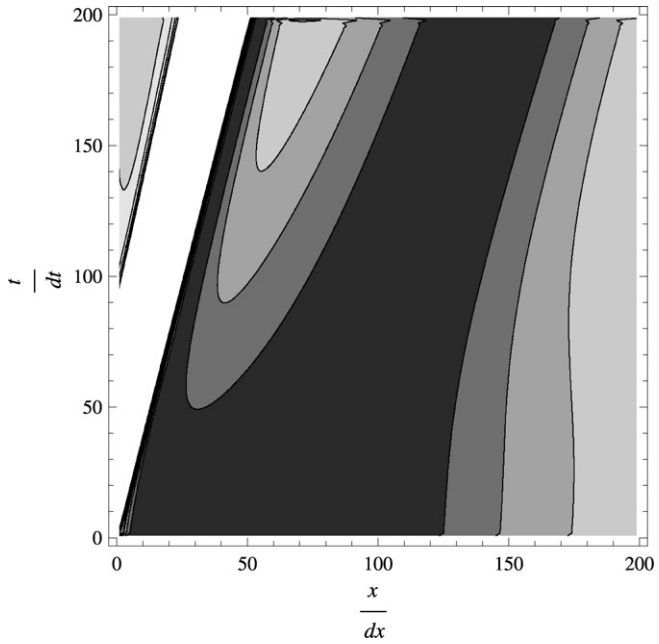

Fig. 5. Isovalues of the residual kinetic energy for the Lax–Wendroff scheme, for $cfl = 0.9$.

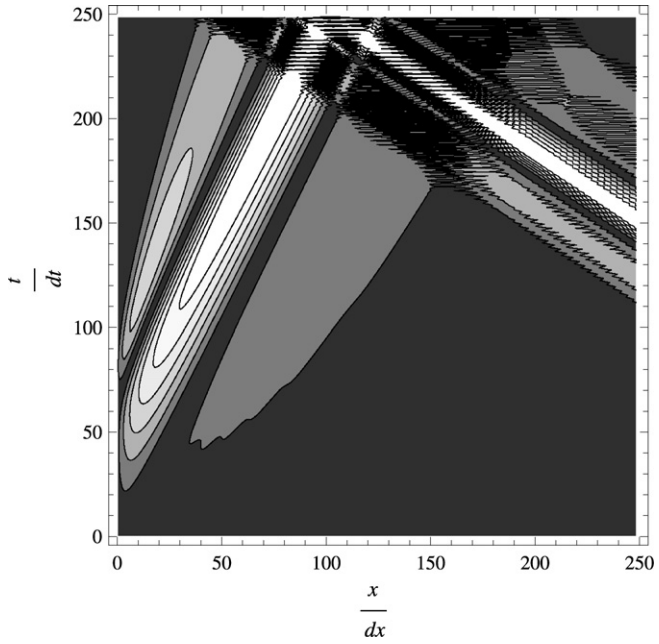

Fig. 6. Isovalues of the residual kinetic energy for the Leapfrog scheme, for $cfl = 0.9$.

Let us now consider the Lax scheme. The dispersion relation is:

$$2e^{i\varphi} + \left\{(\sigma - 1)e^{2\varphi} - (\sigma + 1)\right\}e^{i\omega\tau} = 0 \tag{24}$$

which yields:

$$e^{\eta_\omega \tau} = \sqrt{\mathrm{Cos}^2[\varphi] + \sigma^2 \mathrm{Sin}^2[\varphi]} \tag{25}$$

$$\xi_\omega \tau = \mathrm{ArcTan}\left[\sigma\ \mathrm{Tan}[\varphi]\right] \tag{26}$$

The group velocity is equal to

$$V_g = \frac{c}{\mathrm{Cos}^2[\varphi] + \sigma^2\,\mathrm{Sin}^2[\varphi]} \tag{27}$$

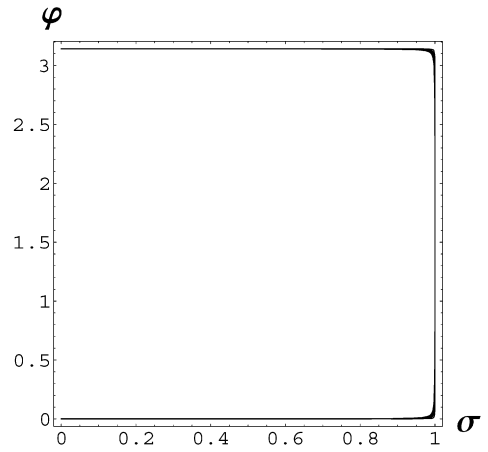

Fig. 7. Roots of Eq. (22), which correspond to possible occurrence of spurious caustics for the Leapfrog scheme.

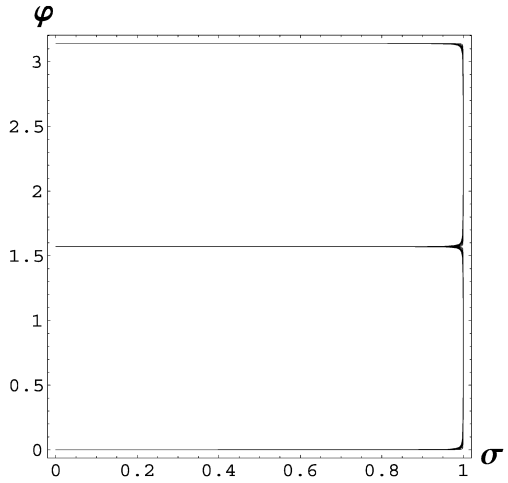

Fig. 8. Roots of Eq. (28), which correspond to possible occurrence of spurious caustics for the Lax scheme.

yielding

$$\frac{\partial V_g}{\partial \varphi} = \frac{2\tau^3(\sigma^2-1)\,\mathrm{Sin}[\varphi]\,\mathrm{Cos}[\varphi]}{\sigma\,(\mathrm{Cos}^2[\varphi]+\sigma^2\,\mathrm{Sin}^2[\varphi])^2} \tag{28}$$

Spurious caustics (see Fig. 8) can arise for $\varphi = 0 \bmod \pi$ and $\varphi = \frac{\pi}{2} \bmod \pi$.

The corresponding group velocities are respectively:

$$U_c{}^1 c, \qquad U_c{}^2 \frac{c}{\sigma^2} \tag{29}$$

For the Lax–Wendroff scheme, the dispersion relation is:

$$2e^{i\varphi} + \sigma(\sigma-1)e^{2i\varphi} - \sigma(\sigma+1) + 2\left(\sigma^2-1\right)e^{i\varphi}e^{i\omega\tau} = 0 \tag{30}$$

which yields:

$$e^{\eta_\omega \tau} = \sqrt{1-4\left(1-\sigma^2\right)\sigma^2\,\mathrm{Sin}^4\left[\frac{\varphi}{2}\right]} \tag{31}$$

$$\xi_\omega \tau = \frac{\sigma\,\mathrm{Sin}[\varphi]}{1-2\sigma^2\,\mathrm{Sin}^2[\frac{\varphi}{2}]} \tag{32}$$

The group velocity is given by

$$V_g = c\frac{\{(1-2\sigma^2\,\mathrm{Sin}^2[\frac{\varphi}{2}])\,\mathrm{Cos}[\varphi]+\sigma^2\,\mathrm{Sin}[\varphi]\,\mathrm{Sin}^2[\frac{\varphi}{2}]\}}{(1-2\sigma^2\,\mathrm{Sin}^2[\frac{\varphi}{2}])^2+\sigma^2\,\mathrm{Sin}[\varphi]^2} \tag{33}$$

from which

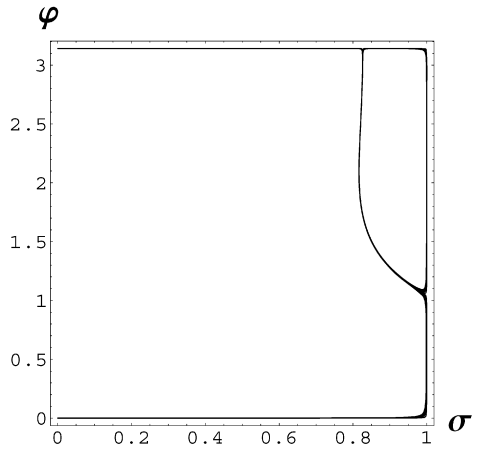

Fig. 9. Roots of (34), which correspond to possible occurrence of spurious caustics for the Lax–Wendroff scheme.

$$\frac{\partial V_g}{\partial \varphi} = -\left\{c^2\tau\left(-1+\sigma^2\right)\left(-2+\sigma^2+3\sigma^4-4\sigma^4\,\mathrm{Cos}[\varphi]\right.\right.$$
$$\left.+\sigma^2\left(-1+\sigma^2\right)\mathrm{Cos}[2\varphi]\right)\mathrm{Sin}[\varphi]\Big\}\Big\{2\sigma\left(\left(1-\sigma^2+\sigma^2\,\mathrm{Cos}[\varphi]\right)^2\right.$$
$$\left.\left.+\sigma^2\,\mathrm{Sin}^2[\varphi]\right)^2\right\}^{-1} \tag{34}$$

Roots of Eq. (34) are shown in Fig. 9.

We finally consider the Crank–Nicolson scheme, whose dispersion relation is:

$$\sigma^2\left(\mathrm{Cos}[\varphi]-1\right)\mathrm{Cos}\left[\frac{\omega\tau}{2}\right] + ic\tau\,\mathrm{Sin}\left[\frac{\omega\tau}{2}\right] = 0 \tag{35}$$

which yields:

$$e^{\eta_\omega\tau} = \frac{\pm(c\tau-2\sigma^2\,\mathrm{Sin}^2[\frac{\varphi}{2}])}{c\tau+2\sigma^2\,\mathrm{Sin}^2[\frac{\varphi}{2}]} \tag{36}$$

$$\xi_\omega\tau = 0 \bmod \pi \tag{37}$$

The group velocity being constant, and therefore no spurious caustics can arise with this scheme.

5. Concluding remarks

The existence of spurious numerical caustics in linear advection schemes has been proved. This linear dispersive phenomenon gives rise to a sudden growth of the L_∞ norm of the error, which corresponds to a local focusing of the numerical error in both space and time. In the present analysis, spurious caustics have been shown to occur in polychromatic solutions.

The energy of the caustic phenomenon depends on the number of spectral modes that will get superimposed at the same time. As a consequence, the spurious error pile-up will be more pronounced in simulations with very small wave-number increments.

It has been shown that most popular existing schemes allow the existence of spurious caustics, while some schemes are caustic-free, like the Crank–Nicolson scheme.

References

[1] D. Bouche, G. Bonnaud, D. Ramos, Comparison of numerical schemes for solving the advection equation, Appl. Math. Lett. 16 (2003).
[2] C. Hirsch, Numerical Computation of Internal and External Flows, Wiley–Interscience, 1988.
[3] B.P. Leonard, A.P. Lock, M.K. Macvean, The NIRVANA scheme applied to one-dimensional advection, Int. J. Numer. Methods Heat Fluid Flow 5 (1995) 341–377.
[4] B.P. Leonard, A.P. Lock, M.K. Macvean, Conservative explicit unrestricted-time-step multidimensional constancy-preserving advection schemes, Monthly Weather Rev. 124 (1996) 2588–2606.

[5] H. Lomax, T.H. Pulliam, D.W. Zingg, Fundamentals of Computational Fluid Dynamics, Springer, 2002.
[6] T.K. Sengupta, Fundamentals of Computational Fluid Dynamics, Hyderabad Univ. Press, 2004.
[7] T.K. Sengupta, A. Dipankar, A comparative study of time advancement methods for solving Navier–Stokes equations, J. Sci. Comput. 21 (2) (2004) 225–250.
[8] T.K. Sengupta, S.K. Sircar, A. Dipankar, High accuracy schemes for DNS and acoustics, J. Sci. Comput. 26 (2) (2006) 151–193.
[9] T.K. Sengupta, A. Dipankar, P. Sagaut, A Fourier–Laplace spectral theory of computing for non-periodic problems: signal and error propagation dynamics, submitted for publication.
[10] R. Vichnevetsky, J.B. Bowles, Fourier analysis of numerical approximations of hyperbolic equations, SIAM Stud. Appl. Math. 5 (1982).
[11] G.B. Witham, Linear and Nonlinear Wave, Wiley–Interscience, 1974.
[12] D.W. Zingg, Comparison of high-accuracy finite-difference methods for linear wave propagation, SIAM J. Sci. Comput. 22 (2000) 227–238.